Available online at www.sciencedirect.com

ScienceDirect

Nuclear and Particle Physics Proceedings 267–269 (2015) 140–149

www.elsevier.com/locate/nppp

Automated Computation of Scattering Amplitudes from Integrand Reduction to Monte Carlo tools

Hans van Deurzen[a], Gionata Luisoni[a], Pierpaolo Mastrolia[a,b], Giovanni Ossola[c,d,*], Zhibai Zhang[c,d]

[a]*Max-Planck Insitut für Physik, Föhringer Ring 6, 80805 München, Germany*
[b]*Dipartimento di Fisica e Astronomia, Università di Padova, and INFN Sezione di Padova, via Marzolo 8, 35131 Padova, Italy*
[c]*Physics Department, New York City College of Technology, The City University of New York, 300 Jay Street Brooklyn, NY 11201, USA*
[d]*The Graduate School and University Center, The City University of New York, 365 Fifth Avenue, New York, NY 10016, USA*

Abstract

After a general introduction about the calculation of one-loop scattering amplitudes via integrand-level techniques, which led to the construction of efficient and automated computational tools for NLO predictions, we briefly describe an approach to the reduction of scattering amplitudes based on integrand-level reduction via multivariate polynomial division also applicable beyond one-loop amplitudes. We also review the main features of the GoSam 2.0 automated framework for NLO calculations and show some of its application to Standard Model processes involving the production massive particles, such as the Higgs boson or top-quark pairs, obtained embedding of the virtual amplitudes produced by GoSam within existing Monte Carlo tools.

Keywords: Scattering Amplitudes, Integrand Reduction, Automation

1. Introduction

The evaluation of scattering amplitudes allows us to test the phenomenological prediction of particle theory with the measurement at collider experiments. By a more abstract point of view, scattering amplitudes can be studied in terms of their symmetries and analytic properties. The understanding of their mathematical structure naturally provides the theoretical framework to develop new techniques for their evaluation, and ultimately to design more efficient computational algorithms for the production of physical cross sections and differential distributions.

Theory predictions play a fundamental role in the particle physics experiments at current hadron colliders. The high luminosity accumulated by the experimental collaborations during the Run-I of the Large Hadron Collider (LHC), allowed for a very detailed investigation of the Standard Model of particle physics. In these analyses, for example to study the properties of the recently discovered Higgs boson [1–4], theoretical predictions are indispensable both for the signal and for the modeling of the relevant background processes, which share similar experimental signatures. Beyond Higgs studies, precise theory predictions allow one to constrain model parameters in the event that a signal of New Physics is detected during the Run-II at the LHC with improved energy.

In this interplay between theoretical prediction and experimental data, it is crucial that the level of productivity of the theory matches the precision of the measurements. Since leading-order (LO) results are affected by large uncertainties, theory predictions are not reliable without accounting for higher orders. Therefore, it is of primary interest to provide theoretical tools which are able to perform the comparison of LHC data to theory at next-to-leading-order (NLO) accuracy.

One of the scopes of this talk is to summarize the recent progress in the evaluation of scattering amplitudes and provide a brief description of integrand-level tech-

*Speaker and Corresponding Author

http://dx.doi.org/10.1016/j.nuclphysbps.2015.10.094

niques, in particular the OPP reduction algorithm, the $d-$dimensional decomposition of scattering amplitudes, and the integrand reduction via multivariate polynomial division.

We will also review the main features of the GoSam framework [5, 6] for the automated computation of one-loop amplitudes and some of the recent results obtained using it. Since the main purpose of GoSam is the computation of the virtual NLO part, in order to produce integrated cross sections and differential distributions it should be interfaced with Monte Carlo (MC) tools. We will focus on this important point in the last part of the talk, where we show some examples of applications.

For a wider outlook on the field, we refer the reader to the plenary presentation of Pierpaolo Mastrolia at this conference [7]. Detailed reports and comprehensive reviews on the different topics described here can be also found in [8–12].

2. Scattering Amplitudes at NLO

The computation of NLO matrix elements requires, in addition to the tree-level LO result, the evaluation of one-loop virtual corrections and contributions from real emission. Both terms are separately infrared (IR) divergent and only their combination leads to a physical result. Moreover, the virtual part is also ultraviolet (UV) divergent, and the UV poles are removed by the renormalization procedure.

While the LO matrix elements and the NLO real parts have been available for a long time, until recently the evaluation of the virtual part of one-loop contributions represented the bottleneck towards the automation of NLO computation. The standard method for the computation of NLO virtual corrections relies on the evaluation of all NLO Feynman diagrams associated with the process. The general task of the calculation is to compute, for each diagram contributing to the amplitude and for each phase space point, the following integral:

$$\mathcal{M} = \int d^d\bar{q}\ \mathcal{A}(\bar{q}) = \int d^d\bar{q} \frac{\mathcal{N}(\bar{q})}{\bar{D}_0\bar{D}_1\dots\bar{D}_{m-1}}\,, \qquad (1)$$

where the $\bar{q}$ denotes integration momenta in $d = 4 - 2\epsilon$ dimensions following the prescription $\bar{q}^2 = q^2 - \mu^2$ and $\bar{D}_i = (\bar{q} + p_i)^2 - m_i^2 = (q + p_i)^2 - \mu^2 - m_i^2$, are accordingly the $d-$dimensional denominators generated by the propagators of the particles inside the loop.

It is well known [13, 14] that the evaluation of the one-loop diagrams can be performed by decomposing each integral $\mathcal{M}$ in terms of a finite set of scalar master integrals (MIs), plus an additional rational function of the masses and momenta appearing in the original amplitude, known in the literature as *rational part* $\mathcal{R}$. The one-loop "master formula" allows to rewrite the integral in Eq. (1) as

$$\begin{aligned}\mathcal{M} \;=\; & \sum_{i_0<i_1<i_2<i_3}^{m-1} \mathbf{d}(\mathbf{i_0 i_1 i_2 i_3}) \int d^d\bar{q}\, \frac{1}{\bar{D}_{i_0}\bar{D}_{i_1}\bar{D}_{i_2}\bar{D}_{i_3}} + \\ & + \sum_{i_0<i_1<i_2}^{m-1} \mathbf{c}(\mathbf{i_0 i_1 i_2}) \int d^d\bar{q}\, \frac{1}{\bar{D}_{i_0}\bar{D}_{i_1}\bar{D}_{i_2}} + \\ & + \sum_{i_0<i_1}^{m-1} \mathbf{b}(\mathbf{i_0 i_1}) \int d^d\bar{q}\, \frac{1}{\bar{D}_{i_0}\bar{D}_{i_1}} + \\ & + \sum_{i_0}^{m-1} \mathbf{a}(\mathbf{i_0}) \int d^d\bar{q}\, \frac{1}{\bar{D}_{i_0}} \;+\; \mathcal{R}\,. \end{aligned} \qquad (2)$$

The calculation of virtual amplitudes can be visualized in terms of three tasks: i) the *generation* of the unintegrated amplitudes $\mathcal{A}$, namely their numerator functions $\mathcal{N}(q)$ and the list of denominators $\bar{D}_i$; ii) the *reduction* of the amplitude to determine all coefficients multiplying each of the MIs in Eq. (2) and the rational term $\mathcal{R}$; iii) the *evaluation of the MIs* which, multiplied by the coefficients obtained in the reduction, provide the final result for the amplitudes. Since in the one-loop case, all scalar master integrals are known and available in public codes [15–19], and amplitudes can be efficiently generated with algebraic or numerical techniques, people mostly focused on the intermediate step, namely the stable and efficient extraction of all the coefficients.

3. Integrand-Reduction Techniques

During the past decade, a powerful framework for one-loop calculation was developed by merging the idea of four-dimensional unitarity-cuts [20, 21], which allow to explore the (poly)logarithmic structure of the amplitudes, with the understanding of the universal algebraic form of any one-loop scattering amplitudes, contained in the OPP method [22–25].

The reduction at the integrand level is based on the decomposition of the numerator function of the amplitude in terms of the propagators that depend on the integration momentum, in order to identify before integration the structures that will generate the scalar integrals and their coefficients and those that will vanish upon integration of the loop momentum. In this approach, the coefficients in front of the MIs can be determined by solving a system of algebraic equations that are obtained by: i) the numerical evaluation of the numerator of the integrand at explicit values of the loop-variable; ii) and the knowledge of the most general polynomial structure of the integrand itself.

The solution of this system of equations becomes particularly simply if we evaluate the expressions for the numerator functions at the set of complex values of the integration momentum for which a given set of inverse propagators vanish, namely the integration momenta corresponding to the so-called quadruple, triple, double, and single cuts. This feature establish a strong connection between the integrand-level techniques and generalized unitarity methods, where the on-shell conditions are imposed at the integral level.

3.1. Integrand-level Reduction in four dimensions

The integral-level reduction algorithm for one-loop scattering amplitudes was originally developed in four dimensions [23–25]. According to this approach, the numerator function $N(q)$ which appears in the integrand for any one-loop scattering amplitudes has a universal, and therefore process-independent, mathematical structure.

Any four-dimensional numerator function $\mathcal{N}(q)$ can be decomposed by reconstructing 4-dimensional denominators $D_i = (q + p_i)^2 - m_i^2$, where q is the integration momentum, and p_i are the linear combinations of the external four-momenta of the incoming and outgoing particles. The q-independent function of masses and external momenta which multiply each group of reconstructed denominators are indeed the set of coefficients which appear in front of the the one-loop scalar functions, that at one loop are the MIs. All other terms in the decomposition that still depend on the integration momentum q are called "spurious terms" because they vanish upon integration and do not contribute to the final result for the scattering amplitude. The universal functional form of such decomposition is process-independent and it is provided in Ref. [23].

In this framework, the task of computing the one-loop amplitude is reduced to the algebraic problem of extracting all the coefficients by evaluating the function $N(q)$ a sufficient number of times at different values of q. This is achieved very efficiently if we employ values of q such that a subset of denominators D_i vanish: such values correspond to the so-called quadruple, triple, double, and single cuts also used in the unitarity-cut method. Operating in this manner, the system of equations becomes triangular. First one determines all the coefficients of the 4-point functions, then moves on to the 3-point coefficients and so on.

This completes the determination of the so-called cut-constructible part, which can be fully achieved in four dimensions. However, as is well known, even starting from a perfectly finite tensor integral, the tensor reduction may lead to integrals that need to be regularized. In dimensional regularization, this is achieved by upgrading the integration momentum to dimension $d = 4 - 2\epsilon$, both in the numerator function and in the set of denominators. Such procedure is responsible for the appearance of the rational part $\mathcal{R}$. Within the OPP approach, the calculation of rational term $\mathcal{R}$ can be split in two separate parts, which have different origins. A first set $\mathcal{R}_1$ appears from the mismatch between the d-dimensional denominators of the master scalar integrals and the 4-dimensional denominators. The term $\mathcal{R}_1$ can be recovered automatically by evaluating the amplitudes for a shifted value of the mass [23]. A second set $\mathcal{R}_2$ comes from the d-dimensionality of the numerator function, and can be recovered by means of *ad hoc* tree-level-like Feynman rules, that are provided in Refs.[25–29] for different models.

Four-dimensional approaches for construction and renormalization of d-dimensional amplitudes have been the target of recent studies. In Ref. [30] a four-dimensional formulation (FDF) of the $d-$dimensional regularization of one-loop scattering amplitude was presented. Within FDF, particles that propagate inside the loop are represented by massive particles regularizing the divergences. Their interactions are described by generalized four-dimensional Feynman rules. More details on this topic are provided in the presentation of William J. Torres Bobadilla [31] at this conference.

The four-dimensional integrand-level reduction algorithm has been implemented in the code CutTools [32], that is publicly available. The method itself does not provide specific recipe for the generation of the numerator function. Some of the early calculations based on CutTools that appeared in the literature [33, 34] employ traditional Feynman diagrams for the generation of the amplitudes. For more advanced applications, CutTools has been incorporated within automated tools for the computation of NLO correction, such as FormCalc [35], Helac-Nlo [36], and MadLoop [37].

3.2. D-dimensional Integrand-level Reduction

Within techniques that operate in four dimensions, the evaluation of the cut-constructible term and the rational term are performed separately, since the latter escapes the four-dimensional detection and its calculation requires information from a different source. Significant improvements in this direction have been achieved employing d-dimensional extension of unitarity methods [38–40], where performing the integrand decomposition in d dimensions, rather than in four, allows for the combined determination of both cut-constructible and rational terms at once [41].

In addition to the standard scalar integrals already contained in the 4-dimensional master formula depicted in Eq. (2), there are additional μ^2-dependent master integrals:

$$\int d^d\bar{q}\frac{\mu^2}{\bar{D}_i\bar{D}_j}\,,\ \int d^d\bar{q}\frac{\mu^2}{\bar{D}_i\bar{D}_j\bar{D}_k}\,,\ \int d^d\bar{q}\frac{\mu^4}{\bar{D}_i\bar{D}_j\bar{D}_k\bar{D}_l}\,,$$

whose expressions are also well-known [42, 43]. The presence of these new contributions, together with the d-dimensional decomposition, account for the complete evaluation of the full rational term.

These ideas were the basis for the development of a new algorithm, called SAMURAI [44], which relies on the extension of the polynomial structures to include an explicit dependence on the extra-dimensional parameter μ needed for the automated computation of the full rational term according to the d-dimensional approach, the parametrization of the residue of the quintuple-cut in terms of the extra-dimension scale [45] and the numerical sampling of the multiple-cut solutions via Discrete Fourier Transform [46].

While the method itself does not provide specific recipe for the generation of the numerator function, SAMURAI can reduce integrands defined either as *numerator functions* sitting on products of denominators, which appear in calculations based on Feynman diagrams, or as *products of tree-level amplitudes* sewn along cut-lines, which is suitable for amplitudes generated with unitarity-based techniques. The reduction provided by SAMURAI has been employed within the GoSam framework, as well as interfaced with FormCalc [47, 48] and within the OpenLoops [49] framework.

The integrand-reduction algorithm was originally developed for cases in which the rank of the numerator function is smaller or equal than the number of external legs (this is indeed the case of renomalizable gauge theories at one-loop). However, this requirement should be lifted to allow for more general models, such as effective theories. In order to deal with the evaluation of $pp \to H + 2,3$ jets in gluon fusion [50, 51], where effective-gluon vertices generated by the large top-mass limit appear and trigger higher rank terms, the reduction code within SAMURAI was upgraded to accommodate such an extension [52–54].

3.3. Integrand Reduction via Laurent Expansion

A different and very powerful approach to integrand reduction was presented [53]. In general, when the multiple-cut conditions do not fully constrain the loop momentum, the on-shell solutions are still functions of some free parameters. The integrand-reduction algorithm as described above requires to solve a system of equations obtained by sampling the numerator on a finite set of values of such free parameters after subtracting all the non-vanishing contributions coming from higher-point residues.

The reduction algorithm can be simplified by exploiting the knowledge of the analytic expression of the integrand. If the analytic form of the numerator is known, all coefficients in the integrand decomposition can be in fact extracted by performing a Laurent expansion with respect to one of the free parameters which appear in the solutions of the cuts.

Moreover, the contributions coming from the subtracted terms can be implemented as analytic corrections to the coefficients, replacing the numerical subtractions of the original algorithm. The parametric form of these corrections can be computed once and for all, in terms of a subset of the higher-point coefficients required by the original algorithm. For instance, box and pentagons do not affect at all the computation of lower-points coefficients.

If either the analytic expression of the integrand or the tensor structure of the numerator is known, the coefficients of the Laurent expansion can be computed, either analytically or numerically, by performing a polynomial division between the numerator and the set of denominators. The method has been implemented in the c++ library NINJA [55]. Its use within the GoSam framework showed an exceptional improvement in the computational performance [56], both in terms of speed and precision, with respect to the standard algorithms. The NINJA library has been already employed in several calculation, among them the evaluation of NLO QCD corrections to $pp \to t\bar{t}Hj$ [57]. It has also been recently interfaced within FormCalc [58].

3.4. Integrand-Level Techniques Beyond One-Loop

Extensions of the integrand-reduction method beyond one-loop, first proposed in Refs. [59, 60], have become the topic of several studies [61–67], thus providing a new direction in the study of multi-loop amplitudes.

Higher-loop techniques require a proper parametrization of the residues at the multi-particle poles [59]. As in the one-loop case, the parametric form of each polynomial residues is process-independent and can be determined once for all from the corresponding multiple cut. However, at higher loops, the basis of MIs is more complicated and so is the form of the residues, which can be written as a multivariate polynomial in the irreducible scalar products (ISP), namely the products that cannot be reconstructed in terms of denominators.

In Refs. [61, 62], the determination of the residues at the multiple cuts has been systematized as a problem

of multivariate polynomial division in algebraic geometry. The use of these techniques proved that the integrand decomposition is applicable not only at one loop, as originally formulated, but at any order in perturbation theory. Moreover, the shape of the residues is uniquely determined by the on-shell conditions, without any additional constraint.

To summarize the algorithm presented in Ref. [62], let us write a general loop integrand as:

$$\mathcal{I}_{i_1\cdots i_n} = \frac{\mathcal{N}_{i_1\cdots i_n}}{\bar{D}_{i_1}\cdots\bar{D}_{i_n}} \,. \tag{3}$$

i) When the on-shell conditions have no solutions, i.e. the number n of denominators $\bar{D}_i$ is larger than the total number of the components of the loop momenta, the integrand $\mathcal{I}_{i_1\cdots i_n}$ is *reducible*: it can be written in terms of lower point functions, namely integrands with $(n-1)$ denominators. This is the case of the six-point functions at one loop.
ii) When the on-shell conditions admit solutions, the corresponding residue is obtained dividing the numerator $\mathcal{N}_{i_1\cdots i_n}$ modulo the Gröbner basis of the n-ple cut. The *remainder* of the division is the *residue* $\Delta_{i_1\cdots i_n}$ of the n-ple cut. The *quotients* generate integrands with $(n-1)$ denominators. Each numerator $\mathcal{N}_{i_1\cdots i_n}$ can be written as:

$$\mathcal{N}_{i_1\cdots i_n} = \sum_{\kappa=1}^{n} \mathcal{N}_{i_1\cdots i_{\kappa-1}i_{\kappa+1}\cdots i_n}\,\bar{D}_{i_\kappa} + \Delta_{i_1\cdots i_n} \,. \tag{4}$$

Using Eq. (3), we get the recurrence relation

$$\mathcal{I}_{i_1\cdots i_n} = \sum_{\kappa=1}^{n} \mathcal{I}_{i_1\cdots i_{\kappa-1}i_{\kappa+1}i_n} + \frac{\Delta_{i_1\cdots i_n}}{\bar{D}_{i_1}\cdots\bar{D}_{i_n}} \,. \tag{5}$$

In this expression the function $\Delta_{i_1\cdots i_n}$ is the residue at the multi-particle pole $\bar{D}_{i_1} = \ldots = \bar{D}_{i_n} = 0$, while $\mathcal{I}_{i_1\cdots i_{\kappa-1}i_{\kappa+1}i_n}$ are integrands with $(n-1)$ denominators that can be further decomposed in lower point functions by applying the same recursive algorithm.

iii) A special set of on-shell cut conditions called *maximum-cuts* are defined by the maximum number of on-shell conditions which can be simultaneously satisfied by the loop momenta. The *Maximum Cut Theorem* [62] ensures that their residues can always be reconstructed by evaluating the numerator at the solutions of the cut, since they are parametrized by exactly n_s coefficients, where n_s is the number of solutions of the multiple cut-conditions. This theorem extends at all orders the features of the one-loop quadruple-cut [21, 23], where the only two complex solutions of the cut determine the two coefficients needed to parametrize the residue.

diagram	Δ	n_s	diagram	Δ	n_s
	c_0	1		$c_0 + c_1 z$	2
	$\sum_{i=0}^{3} c_i z^i$	4		$\sum_{i=0}^{3} c_i z^i$	4
	$\sum_{i=0}^{7} c_i z^i$	8	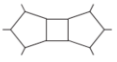	$\sum_{i=0}^{7} c_i z^i$	8

Figure 1: Examples of maximum-cuts.

In Figure 1, we show the structures of the residues of the maximum cut, together with the corresponding values of n_s, for a selection of diagrams with different number of loops (one, two, and three). With the exception of the first diagram in the left column, which represents the 5-ple cut of the 5-point one-loop dimensionally regulated amplitude, all the other diagrams in the table are considered in four dimensions. For each of them, the general structure of the residue Δ and the corresponding value of n_s are provided. Similar conditions can be found for more complicated topologies at higher loops.

The integrand recurrence relation of Eq. (5) can be applied in two different ways. After the parametric form of all residues has been determined, if the solutions of all multiple cuts are known, the coefficients which appear in the residues can be determined by evaluating the numerator at the solutions of the multiple cuts, as many times as the number of the unknown coefficients. This approach has been employed at one loop in the original integrand reduction [23], and the language of multivariate polynomial division provides its generalization at all loops.

As a very different strategy [67], the decomposition can be obtained analytically by successive polynomial divisions. In this approach, the reduction algorithm is applied directly to the actual numerator functions, without requiring the knowledge of the parametric form of all residues or the solutions of the multiple cuts. In Ref. [67], we showed how this strategy can be successfully applied to integrands with denominators appearing with multiple powers, thus solving a long-standing problem within unitarity-based methods.

4. Virtual NLO with GoSam 2.0

The idea behind the GoSam framework is to combine automated diagram generation and algebraic manipu-

lation [68–71] with the integrand-level reduction techniques described above. Amplitudes are automatically generated via Feynman diagrams, so that the only task required from the user is the preparation of an input file for the generation of the code, without having to worry about the internal details.

We recently released GoSam 2.0, a new version of the code that offers numerous improvements both on the generation and the reduction side, resulting in faster and more stable codes for calculations within and beyond the Standard Model. After the generation of all contributing diagrams, the virtual corrections are evaluated using the integrand reduction via Laurent expansion provided by Ninja, or the d-dimensional integrand-level reduction method, as implemented in Samurai. Alternatively, the tensorial decomposition provided by Golem95C [72, 73] is also available. GoSam 2.0 can be used to generate and evaluate one-loop corrections in both QCD and electro-weak theory. Model files for Beyond Standard Model (BSM) applications can be generated from a Universal FeynRules Output (UFO) [74, 75] or with LanHEP [76].

The code has been employed in several applications at NLO QCD accuracy [50, 51, 57, 77–81], studies of BSM scenarios [82–84], electroweak calculations [85, 86], and recently also within NNLO calculations for the production of real-virtual contributions [87–89].

GoSam 2.0 also contains the extended version of the standardized *Binoth Les Houches Accord* (BLHA) interface [90, 91] to Monte Carlo programs.

5. Production of physical results at NLO precision, interfaces with Monte Carlo tools

The computation of physical observables at NLO accuracy, such as cross sections and differential distributions, requires to combine the one-loop results for the virtual amplitudes obtained with GoSam, with other tools that can take care of the computation of the real emission contributions and of the subtraction terms, needed to control the cancellation of IR singularities. This can be obtained by embedding the calculation of virtual corrections within a Monte Carlo framework (MC), that can provide the phase-space integration, and of the combination of the different pieces of the calculation. A complete table of GoSam's interfaces with MC programs has been recently presented in [92].

At present, the GoSam code has been successfully interfaced with several Monte Carlo tools, in order to provide insightful phenomenological applications [93–95]. While in the following we will show examples obtained within the frameworks of Sherpa [96] and aMC@NLO [97], results have been also obtained within the Herwig++/Matchbox [98], whizard [99], and Powheg [100] frameworks.

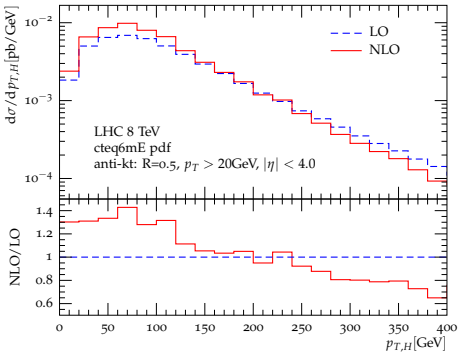

Figure 2: $pp \to H + 3j$ in GF for the LHC at 8 TeV: transverse momentum distribution of the Higgs boson at LO and NLO.

Higgs boson production in Gluon Fusion. The extension of integrand reduction to allow for higher rank integrands, described in Section 3.2, allowed us to compute the NLO QCD corrections to the production of $H + 2$ jets [50] and, for the first time, also $H + 3$ jets [51] in Gluon Fusion in the large top-mass limit. This calculation is indeed challenging both on the side of real-emission contributions and of the virtual corrections, which alone involve more than ten thousand one-loop Feynman diagrams with up to rank-seven hexagons. Due to the complexity of the integration, for the results presented in Ref. [51] we employed a hybrid setup which combines GoSam, Sherpa and the MadDipole/Madgraph4/MadEvent framework [101–105]. The p_T distribution for the Higgs boson in Fig. 2 shows how the NLO corrections enhance all distributions for p_T values lower than $150 - 200$ GeV, whereas their contribution is negative at higher p_T.

An updated analysis appeared in the "Physics at TeV Colliders: Standard Model Working Group Report" [12], which contains new results and distributions for $H + 3$ jets at NLO for a set of ATLAS-like cuts and a comparison with the NLO predictions for $H + 2$ jets (see Fig. 3), including the three-to-two jet cross section ratio at LO and NLO. Further studies for Higgs plus jets production are currently in progress, which contain the analysis of the effects of different cuts, merging with smaller multiplicities, and matching with parton shower.

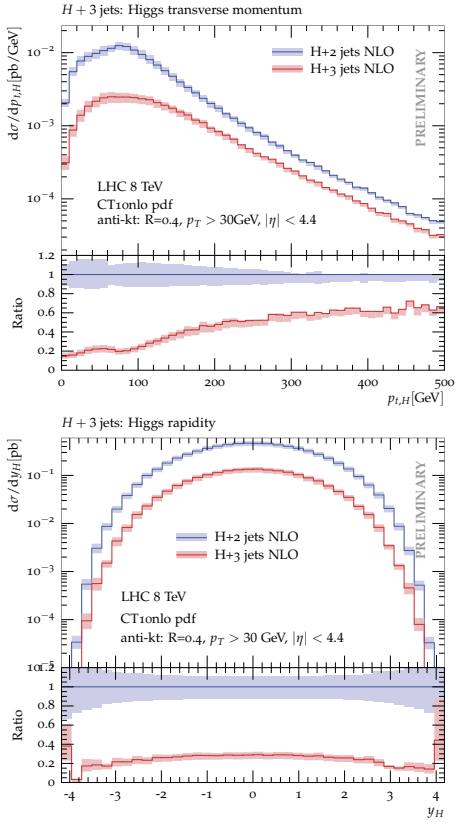

Figure 3: $pp \to H + 3j$ in GF for the LHC at 8 TeV: distributions of NLO transverse momentum and rapidity of the Higgs boson compared with the NLO prediction for $pp \to H + 2j$.

NLO QCD corrections to $pp \to t\bar{t}Hj$. The production rate for a Higgs boson associated with a top-antitop pair is particularly interesting to study the coupling of the Higgs boson to the top quark. In Ref. [57], we presented the calculation of the complete NLO QCD corrections to the process $pp \to t\bar{t}H + 1$ jet at the LHC, which is important for the phenomenological analyses at the LHC, in particular for the high-p_T region, where the presence of the additional jet can be relevant. As an illustration, in Fig. 4, we report the distribution of the top-pair invariant mass. This process is also challenging by a technical point of view for the presence of two mass scales, Higgs boson and top quark, in addition to a high number of diagrams. Indeed, this calculation represented the first application and validation of the reduction algorithm described in Section 3.3.

Further analyses for $pp \to t\bar{t}H + 0, 1$ jets are currently in progress.

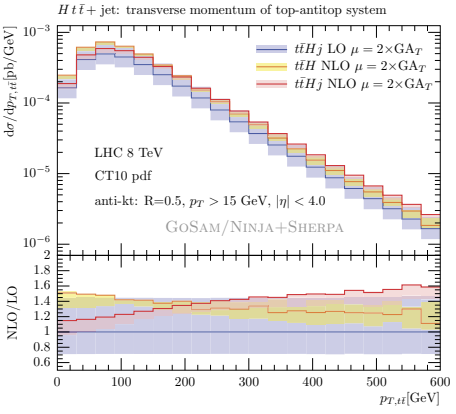

Figure 4: Transverse momentum of the top-quark pair in $pp \to t\bar{t}Hj$.

GoSam+*a*MC@NLO *vs* GoSam+Sherpa. As a last example of application of GoSam 2.0, we show a comparison between the NLO differential distributions obtained interfacing it with two different multi-purpose Monte Carlo tools. As a benchmark process, we studied the $t\bar{t}H$ production at the 8 TeV-LHC, with a fixed scale $\mu = 2m_T + m_H$, and `CT10nlo` PDF set. Among the several distributions that we checked, some examples are presented in Fig. 5 and Fig. 6 . The agreement between the results obtained with the two tools is remarkably good.

A detailed work which contains a description of the interface between GoSam and aMC@NLO, together with phenomenological studies of $pp \to t\bar{t}\gamma\gamma$, is currently in progress [106].

6. Conclusions and Future Outlook

The study of scattering amplitudes provides a fertile ground for many theoretical applications. The developments of the past decade show how a better understanding of mathematical properties of scattering amplitudes can provide the basis for the construction of efficient algorithms for their evaluation, and ultimately leads to higher quality predictions to be used in the experimental analyses at the particle colliders. As of today, several different approaches available for one-loop calculations, which are encoder in different computational tools and interfaced with Monte Carlo event generators, to provide NLO predictions for a variety of processes needed by the LHC experimental collaborations.

In this presentation, we reviewed the main features of the integrand reduction techniques, described some of the algorithms for the evaluation of scattering amplitudes that can be constructed following those ideas, and

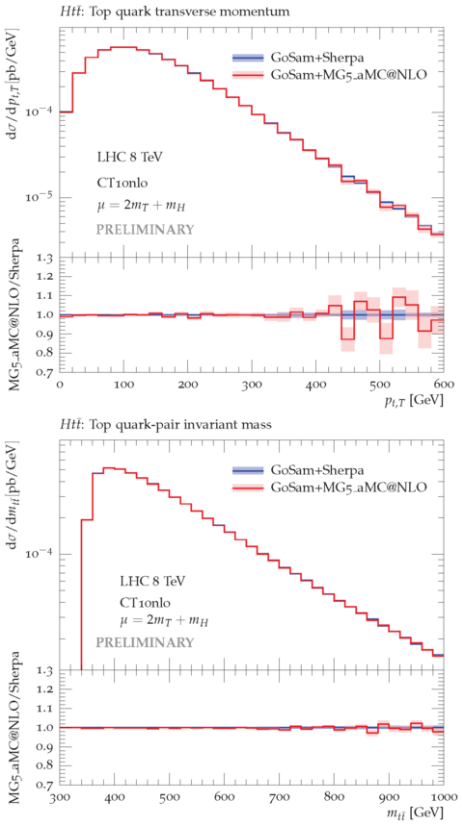

Figure 5: Comparison GoSam+aMC@NLO vs GoSam+Sherpa, $pp \to t\bar{t}H$ for the LHC at 8 TeV: transverse momentum of the top quark and invariant mass of the $t\bar{t}$ pair.

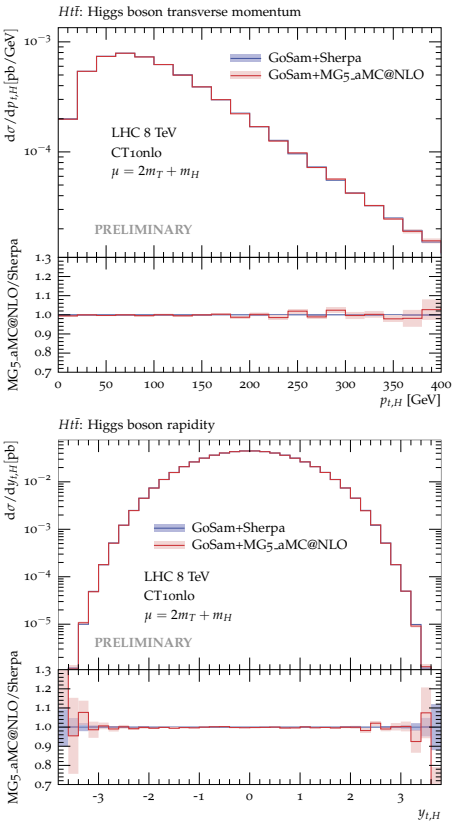

Figure 6: Comparison GoSam+aMC@NLO vs GoSam+Sherpa, $pp \to t\bar{t}H$ for the LHC at 8 TeV: transverse momentum of the Higgs boson, and Higgs boson rapidity.

showed their application in a selection of phenomenological studies for the 8 TeV-LHC, obtained within the GoSam framework.

The GoSam 2.0 release contains several improvements respect to its earlier versions. GoSam established itself as a flexible and widely applicable tool for the automated calculation of the virtual part of multi-particle scattering amplitudes at NLO accuracy and provides a reliable answer for multi-leg amplitudes in the presence of massive internal and external legs and propagators. Recent examples of calculations performed with GoSam include NLO QCD corrections to Higgs production channels and backgrounds, neutralino and graviton production in BSM scenarios, and electroweak corrections. The code has also been employed for the evaluation of the real-virtual part within NNLO calculations.

Several new NLO analyses are currently under way, which exploit the combination of GoSam, as provider of one-loop virtual amplitudes, within the flexible framework of Monte Carlo event generators. Such interfaces should be improved and simplified, to allow for an automated generation of analyses which include parton shower effect and the merging of different multiplicities, as needed by comparisons with experimental data.

Looking ahead, as the focus is shifting towards the challenges presented by NNLO calculations, new ideas and techniques [107–111], along with improved version of known algorithms, are starting to make an impact. In this context, it will be interesting to observe whether the extensions of integrand-level techniques to higher orders will succeed to provide a comparable level of reliability, and eventually of automation, as in the one-loop case, and to what extent the GoSam framework could be extended to explore the new frontiers in precision calculations.

Acknowledgments. We would like to thank the present and former members of the GoSam Collaboration for their contributions to the results presented in this talk. H.v.D., G.L., and P.M. are supported by the Alexan-

der von Humboldt Foundation, in the framework of the Sofja Kovaleskaja Award Project Advanced Mathematical Methods for Particle Physics, endowed by the German Federal Ministry of Education and Research. The work of G.O. and Z.Z. was supported in part by the National Science Foundation under Grant PHY-1068550 and PSC-CUNY Award No. 65188-00 43. G.O. also acknowledges the support of NSF under Grant PHY-1417354. The authors are grateful to the Center for Theoretical Physics of New York City College of Technology for providing computational resources.

References

[1] Englert F and Brout R 1964 *Phys.Rev.Lett.* **13** 321–323
[2] Higgs P W 1964 *Phys.Lett.* **12** 132–133
[3] Aad G *et al.* (ATLAS Collaboration) 2012 *Phys.Lett.* **B716** 1–29 (*Preprint* 1207.7214)
[4] Chatrchyan S *et al.* (CMS Collaboration) 2012 *Phys.Lett.* **B716** 30–61 (*Preprint* 1207.7235)
[5] Cullen G, Greiner N, Heinrich G, Luisoni G, Mastrolia P *et al.* 2012 *Eur.Phys.J.* **C72** 1889 (*Preprint* 1111.2034)
[6] Cullen G, van Deurzen H, Greiner N, Heinrich G, Luisoni G *et al.* 2014 *Eur.Phys.J.* **C74** 3001 (*Preprint* 1404.7096)
[7] Mastrolia P *Plenary Talk at SILAFAE X, in these proceedings*
[8] Bern Z, Dixon L J and Kosower D A 2007 *Annals Phys.* **322** 1587–1634 (*Preprint* 0704.2798)
[9] Ellis R K, Kunszt Z, Melnikov K and Zanderighi G 2012 *Phys.Rept.* **518** 141–250 (*Preprint* 1105.4319)
[10] Ossola G 2014 *J.Phys.Conf.Ser.* **523** 012040 (*Preprint* 1310.3214)
[11] Heinemeyer S *et al.* (The LHC Higgs Cross Section Working Group) 2013 (*Preprint* 1307.1347)
[12] Butterworth J, Dissertori G, Dittmaier S, de Florian D, Glover N *et al.* 2014 (*Preprint* 1405.1067)
[13] Passarino G and Veltman M J G 1979 *Nucl. Phys.* **B160** 151
[14] 't Hooft G and Veltman M 1979 *Nucl.Phys.* **B153** 365–401
[15] van Oldenborgh G 1991 *Comput.Phys.Commun.* **66** 1–15
[16] Hahn T and Perez-Victoria M 1999 *Comput.Phys.Commun.* **118** 153–165 (*Preprint* hep-ph/9807565)
[17] Ellis R K and Zanderighi G 2008 *JHEP* **02** 002 (*Preprint* 0712.1851)
[18] van Hameren A 2011 *Comput.Phys.Commun.* **182** 2427–2438 (*Preprint* 1007.4716)
[19] Cullen G, Guillet J, Heinrich G, Kleinschmidt T, Pilon E *et al.* 2011 *Comput.Phys.Commun.* **182** 2276–2284 (*Preprint* 1101.5595)
[20] Bern Z, Dixon L J, Dunbar D C and Kosower D A 1994 *Nucl. Phys.* **B425** 217–260 (*Preprint* hep-ph/9403226)
[21] Britto R, Cachazo F and Feng B 2005 *Nucl. Phys.* **B725** 275–305 (*Preprint* hep-th/0412103)
[22] del Aguila F and Pittau R 2004 *JHEP* **0407** 017 (*Preprint* hep-ph/0404120)
[23] Ossola G, Papadopoulos C G and Pittau R 2007 *Nucl.Phys.* **B763** 147–169 (*Preprint* hep-ph/0609007)
[24] Ossola G, Papadopoulos C G and Pittau R 2007 *JHEP* **0707** 085 (*Preprint* 0704.1271)
[25] Ossola G, Papadopoulos C G and Pittau R 2008 *JHEP* **0805** 004 (*Preprint* 0802.1876)
[26] Draggiotis P, Garzelli M, Papadopoulos C and Pittau R 2009 *JHEP* **0904** 072 (*Preprint* 0903.0356)
[27] Garzelli M, Malamos I and Pittau R 2011 *JHEP* **1101** 029 (*Preprint* 1009.4302)
[28] Garzelli M and Malamos I 2011 *Eur.Phys.J.* **C71** 1605 (*Preprint* 1010.1248)
[29] Page B and Pittau R 2013 *JHEP* **1309** 078 (*Preprint* 1307.6142)
[30] Fazio R A, Mastrolia P, Mirabella E and Torres Bobadilla W J 2014 *Eur.Phys.J.* **C74** 3197 (*Preprint* 1404.4783)
[31] Torres Bobadilla W J *Presentation at SILAFAE X, in these proceedings*
[32] Ossola G, Papadopoulos C G and Pittau R 2008 *JHEP* **03** 042 (*Preprint* 0711.3596)
[33] Binoth T, Ossola G, Papadopoulos C and Pittau R 2008 *JHEP* **0806** 082 (*Preprint* 0804.0350)
[34] Actis S, Mastrolia P and Ossola G 2010 *Phys.Lett.* **B682** 419–427 (*Preprint* 0909.1750)
[35] Hahn T 2008 *PoS* **ACAT08** 121 (*Preprint* 0901.1528)
[36] Bevilacqua G, Czakon M, Garzelli M, van Hameren A, Kardos A *et al.* 2013 *Comput.Phys.Commun.* **184** 986–997 (*Preprint* 1110.1499)
[37] Hirschi V, Frederix R, Frixione S, Garzelli M V, Maltoni F *et al.* 2011 *JHEP* **1105** 044 (*Preprint* 1103.0621)
[38] Ellis R K, Giele W T and Kunszt Z 2008 *JHEP* **03** 003 (*Preprint* 0708.2398)
[39] Giele W T, Kunszt Z and Melnikov K 2008 *JHEP* **0804** 049 (*Preprint* 0801.2237)
[40] Ellis R, Giele W T, Kunszt Z and Melnikov K 2009 *Nucl.Phys.* **B822** 270–282 (*Preprint* 0806.3467)
[41] Giele W and Zanderighi G 2008 *JHEP* **0806** 038 (*Preprint* 0805.2152)
[42] Pittau R 1997 *Comput. Phys. Commun.* **104** 23–36 (*Preprint* hep-ph/9607309)
[43] Bern Z and Morgan A G 1996 *Nucl. Phys.* **B467** 479–509 (*Preprint* hep-ph/9511336)
[44] Mastrolia P, Ossola G, Reiter T and Tramontano F 2010 *JHEP* **1008** 080 (*Preprint* 1006.0710)
[45] Melnikov K and Schulze M 2010 *Nucl.Phys.* **B840** 129–159 (*Preprint* 1004.3284)
[46] Mastrolia P, Ossola G, Papadopoulos C and Pittau R 2008 *JHEP* **0806** 030 (*Preprint* 0803.3964)
[47] Agrawal S, Hahn T and Mirabella E 2012 *J.Phys.Conf.Ser.* **368** 012054 (*Preprint* 1112.0124)
[48] Nejad B C, Hahn T, Lang J N and Mirabella E 2013 (*Preprint* 1310.0274)
[49] Cascioli F, Maierhofer P and Pozzorini S 2012 *Phys.Rev.Lett.* **108** 111601 (*Preprint* 1111.5206)
[50] van Deurzen H, Greiner N, Luisoni G, Mastrolia P, Mirabella E *et al.* 2013 *Phys.Lett.* **B721** 74–81 (*Preprint* 1301.0493)
[51] Cullen G, van Deurzen H, Greiner N, Luisoni G, Mastrolia P *et al.* 2013 *Phys.Rev.Lett.* **111** 131801 (*Preprint* 1307.4737)
[52] Mastrolia P, Mirabella E, Ossola G, Peraro T and van Deurzen H 2012 *PoS* **LL2012** 028 (*Preprint* 1209.5678)
[53] Mastrolia P, Mirabella E and Peraro T 2012 *JHEP* **1206** 095 (*Preprint* 1203.0291)
[54] van Deurzen H 2013 *Acta Phys.Polon.* **B44** 2223–2230
[55] Peraro T 2014 *Comput.Phys.Commun.* **185** 2771–2797 (*Preprint* 1403.1229)
[56] van Deurzen H, Luisoni G, Mastrolia P, Mirabella E, Ossola G *et al.* 2014 *JHEP* **1403** 115 (*Preprint* 1312.6678)
[57] van Deurzen H, Luisoni G, Mastrolia P, Mirabella E, Ossola G *et al.* 2013 *Phys.Rev.Lett.* **111** 171801 (*Preprint* 1307.8437)
[58] Gro C, Hahn T, Heinemeyer S, von der Pahlen F, Rzehak H *et al.* 2014 (*Preprint* 1407.0235)
[59] Mastrolia P and Ossola G 2011 *JHEP* **1111** 014 (*Preprint* 1107.6041)

[60] Badger S, Frellesvig H and Zhang Y 2012 *JHEP* **1204** 055 (*Preprint* 1202.2019)
[61] Zhang Y 2012 *JHEP* **1209** 042 (*Preprint* 1205.5707)
[62] Mastrolia P, Mirabella E, Ossola G and Peraro T 2012 *Phys.Lett.* **B718** 173–177 (*Preprint* 1205.7087)
[63] Kleiss R H, Malamos I, Papadopoulos C G and Verheyen R 2012 *JHEP* **1212** 038 (*Preprint* 1206.4180)
[64] Badger S, Frellesvig H and Zhang Y 2012 *JHEP* **1208** 065 (*Preprint* 1207.2976)
[65] Feng B and Huang R 2013 *JHEP* **1302** 117 (*Preprint* 1209.3747)
[66] Mastrolia P, Mirabella E, Ossola G and Peraro T 2013 *Phys.Rev.* **D87** 085026 (*Preprint* 1209.4319)
[67] Mastrolia P, Mirabella E, Ossola G and Peraro T 2013 *Phys.Lett.* **B727** 532–535 (*Preprint* 1307.5832)
[68] Nogueira P 1993 *J.Comput.Phys.* **105** 279–289
[69] Vermaseren J A M 2000 (*Preprint* math-ph/0010025)
[70] Reiter T 2010 *Comput.Phys.Commun.* **181** 1301–1331 (*Preprint* 0907.3714)
[71] Cullen G, Koch-Janusz M and Reiter T 2011 *Comput.Phys.Commun.* **182** 2368–2387 (*Preprint* 1008.0803)
[72] Binoth T, Guillet J P, Heinrich G, Pilon E and Reiter T 2009 *Comput.Phys.Commun.* **180** 2317–2330 (*Preprint* 0810.0992)
[73] Heinrich G, Ossola G, Reiter T and Tramontano F 2010 *JHEP* **1010** 105 (*Preprint* 1008.2441)
[74] Degrande C, Duhr C, Fuks B, Grellscheid D, Mattelaer O *et al.* 2012 *Comput.Phys.Commun.* **183** 1201–1214 (*Preprint* 1108.2040)
[75] Alloul A, Christensen N D, Degrande C, Duhr C and Fuks B 2014 *Comput.Phys.Commun.* **185** 2250–2300 (*Preprint* 1310.1921)
[76] Semenov A 2014 (*Preprint* 1412.5016)
[77] Greiner N, Guffanti A, Reiter T and Reuter J 2011 *Phys.Rev.Lett.* **107** 102002 (*Preprint* 1105.3624)
[78] Greiner N, Heinrich G, Mastrolia P, Ossola G, Reiter T *et al.* 2012 *Phys.Lett.* **B713** 277–283 (*Preprint* 1202.6004)
[79] Gehrmann T, Greiner N and Heinrich G 2013 *JHEP* **1306** 058 (*Preprint* 1303.0824)
[80] Gehrmann T, Greiner N and Heinrich G 2013 (*Preprint* 1308.3660)
[81] Dolan M J, Englert C, Greiner N and Spannowsky M 2013 (*Preprint* 1310.1084)
[82] Cullen G, Greiner N and Heinrich G 2013 *Eur.Phys.J.* **C73** 2388 (*Preprint* 1212.5154)
[83] Greiner N, Heinrich G, Reichel J and von Soden-Fraunhofen J F 2013 *JHEP* **1311** 028 (*Preprint* 1308.2194)
[84] Greiner N, Kong K, Park J C, Park S C and Winter J C 2014 (*Preprint* 1410.6099)
[85] Chiesa M, Montagna G, Barze' L, Moretti M, Nicrosini O *et al.* 2013 *Phys.Rev.Lett.* **111** 121801 (*Preprint* 1305.6837)
[86] Mishra K, Becher T, Barze L, Chiesa M, Dittmaier S *et al.* 2013 (*Preprint* 1308.1430)
[87] Gao J and Zhu H X 2014 *Phys.Rev.* **D90** 114022 (*Preprint* 1408.5150)
[88] Gao J and Zhu H X 2014 *Phys.Rev.Lett.* **113** 262001 (*Preprint* 1410.3165)
[89] Del Duca V, Duhr C, Somogyi G, Tramontano F and Trocsanyi Z 2015 (*Preprint* 1501.07226)
[90] Binoth T, Boudjema F, Dissertori G, Lazopoulos A, Denner A *et al.* 2010 *Comput.Phys.Commun.* **181** 1612–1622 (*Preprint* 1001.1307)
[91] Alioli S, Badger S, Bellm J, Biedermann B, Boudjema F *et al.* 2013 (*Preprint* 1308.3462)
[92] van Deurzen H, Greiner N, Heinrich G, Luisoni G, Mirabella E *et al.* 2014 *PoS* **LL2014** 021 (*Preprint* 1407.0922)
[93] Luisoni G, Nason P, Oleari C and Tramontano F 2013 *JHEP* **1310** 083 (*Preprint* 1306.2542)
[94] Hoeche S, Huang J, Luisoni G, Schoenherr M and Winter J 2013 *Phys.Rev.* **D88** 014040 (*Preprint* 1306.2703)
[95] Luisoni G, Oleari C and Tramontano F 2015 (*Preprint* 1502.01213)
[96] Gleisberg T, Hoeche S, Krauss F, Schonherr M, Schumann S *et al.* 2009 *JHEP* **0902** 007 (*Preprint* 0811.4622)
[97] Alwall J, Frederix R, Frixione S, Hirschi V, Maltoni F *et al.* 2014 *JHEP* **1407** 079 (*Preprint* 1405.0301)
[98] Bellm J, Gieseke S, Grellscheid D, Papaefstathiou A, Platzer S *et al.* 2013 (*Preprint* 1310.6877)
[99] Reuter J, Bach F, Chokoufe B, Kilian W, Ohl T *et al.* 2014 (*Preprint* 1410.4505)
[100] Alioli S, Nason P, Oleari C and Re E 2010 *JHEP* **1006** 043 (*Preprint* 1002.2581)
[101] Frederix R, Gehrmann T and Greiner N 2008 *JHEP* **0809** 122 (*Preprint* 0808.2128)
[102] Frederix R, Gehrmann T and Greiner N 2010 *JHEP* **1006** 086 (*Preprint* 1004.2905)
[103] Stelzer T and Long W 1994 *Comput.Phys.Commun.* **81** 357–371 (*Preprint* hep-ph/9401258)
[104] Maltoni F and Stelzer T 2003 *JHEP* **0302** 027 (*Preprint* hep-ph/0208156)
[105] Alwall J, Demin P, de Visscher S, Frederix R, Herquet M *et al.* 2007 *JHEP* **0709** 028 (*Preprint* 0706.2334)
[106] van Deurzen H, Frederix R, Hirschi V, Luisoni G, Mastrolia P and Ossola G *In preparation*
[107] Henn J M 2013 *Phys.Rev.Lett.* **110** 251601 (*Preprint* 1304.1806)
[108] Argeri M, Di Vita S, Mastrolia P, Mirabella E, Schlenk J *et al.* 2014 *JHEP* **1403** 082 (*Preprint* 1401.2979)
[109] Papadopoulos C G 2014 *JHEP* **1407** 088 (*Preprint* 1401.6057)
[110] Gehrmann T, von Manteuffel A, Tancredi L and Weihs E 2014 *JHEP* **1406** 032 (*Preprint* 1404.4853)
[111] Lee R N 2014 (*Preprint* 1411.0911)